Available online at www.sciencedirect.com

SciVerse ScienceDirect

Scripta Materialia 68 (2013) 87–90

Scripta MATERIALIA

www.elsevier.com/locate/scriptamat

The thermal cycle during the dissimilar friction spot welding of aluminum and magnesium alloy

U.F.H. Suhuddin,* V. Fischer and J.F. dos Santos

Helmholtz-Zentrum Geesthacht, Institute of Materials Research, Materials Mechanics, Solid-State Joining Processes, Max-Planck-Str. 1, 21502 Geesthacht, Germany

Received 24 August 2012; revised 13 September 2012; accepted 13 September 2012
Available online 21 September 2012

The thermal cycle during dissimilar friction spot welding of Al alloy AA5754 to Mg alloy AZ31 was measured by thermocouples located in the weld region. The results revealed that the weld is exposed to a non-equilibrium solidus temperature induced by rapid heating and cooling. Microstructural analyses showed that the grain structure development in the stir zone was affected by grain boundary diffusion, interfacial diffusion and dynamic recrystallization, which resulted in fine equiaxed grains of $Al_{12}Mg_{17}$ in the weld center.

Keywords: Friction spot welding; Peak temperature; Solidus temperature; Intermetallic compound; Diffusion

Friction spot welding (FSpW), also known as refill friction stir spot welding, is one of the friction stir welding (FSW) process variants capable of joining two or more materials in a spot-like lap joint configuration [1]. FSpW uses a non-consumable tool consisting of three independent movable parts, including two rotating parts, the sleeve and the pin, and a stationary clamping ring. A schematic illustration of the process is shown in Figure 1. The stationary clamping ring holds the materials against the backing bar, while the rotating sleeve plunges downward into the material, and the pin moves in the reverse direction. The rotating sleeve introduces plastic deformation and generates frictional heating, thereby plasticizing the materials. The sleeve squeezes the softening materials, filling the cavity left by the pin. Then, the rotating sleeve and the pin move back to their initial positions, pushing the softened material into the joint. Finally, the tool is retracted from the surface, leaving the weld without a keyhole. Due to the advantages of this technique, such as the resulting good mechanical properties and the keyhole-free surface [2,3], FSpW has been successfully used for joining similar welds of Al or Mg alloys [2,3] and has been considered for use in joining dissimilar Al and Mg alloys.

Several studies have shown that the dissimilar friction-based joining of Al and Mg alloys can lead to the formation of intermetallic compounds (IMCs), such as $Al_{12}Mg_{17}$ [4–7], Al_3Mg_2 [6,7] and Mg_2Si [7]. Several attempts [4,5] have been made to clarify the peak temperature achieved during dissimilar friction-based joining processes to understand the formation of IMCs. Sato et al. [4] suggested that the peak temperature should be higher than 460 °C, based on the measurements of similar FSW processes applied to AA1050 and AZ31. The intensive mutual diffusion at the weld center comprising alternating bands of Al and Mg alloys can lead to a formation of a constitutional liquid phase when the material is constantly held at temperatures higher than 460 °C. Meanwhile, Gerlich et al. [5] measured the temperature in dissimilar Al/Mg spot welds by embedding a thermocouple inside the tool. They suggested that the formation of a eutectic liquid adjacent to the pin stabilizes the temperature at 437 °C, which corresponds to the solidus temperature.

The present study investigates the thermal cycle during the dissimilar FSpW of AA5754 and AZ31 by embedding thermocouples in the joint area, as illustrated in Figure 1. Because no part of the tool plunges into the weld center during FSpW, the thermal disruption that arises from contact between the tool and the thermocouple is negligible.

The materials used for welding were 2 mm thick Al alloy AA5754 and Mg alloy AZ31 sheets, which have

* Corresponding author. Tel.: +49 4152 87 2070; fax: +49 4152 87 2033; e-mail: uceu.suhuddin@hzg.de

1359-6462/$ - see front matter © 2012 Acta Materialia Inc. Published by Elsevier Ltd. All rights reserved.
http://dx.doi.org/10.1016/j.scriptamat.2012.09.008

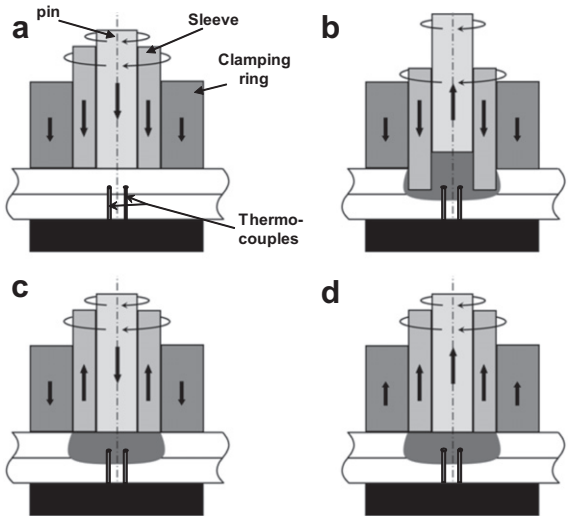

Figure 1. A schematic illustration of the friction spot welding process and the thermocouple placement during the temperature measurements.

nominal chemical compositions, as shown in Table 1. The process was performed using a tool with component dimensions of 14.5, 9 and 6 mm in diameter for the clamping ring, the sleeve and the pin, respectively. During welding, the Al sheet was placed on top of the Mg sheet. The welding parameters included a tool rotational speed of 1900 rpm, a sleeve plunge depth of 1.6 mm, a dwell time of 2 s and a clamping force of 12 kN. The sleeve plunging and retracting speeds were 0.8 mm s^{-1}. At the end of the process, the sleeve and the pin were maintained in the rotating state on the surface for 1 s to improve the weld appearance. The temperature measurements were carried out for three welds to assure the repeatability of the thermal cycle data. Two K-type thermocouples were embedded in the Al sheet, at a depth of 2.5 mm from the bottom of the Mg sheet, as illustrated in Figure 1. The temperature values were recorded at a frequency of 50 Hz. To obtain more insight into the grain structure, additional "stop action" experiments were carried out. In the "stop action" experiments, the welding cycle was forced to stop during the dwell period; subsequently, a mixture of ice and water was poured to freeze the microstructure, hereafter referred to as a "quenched sample."

For the microstructural analysis, the welds were sectioned across the weld center, then ground and polished. The microstructural analyses were carried out using an optical microscope and a scanning electron microscope (SEM) equipped with an energy dispersive X-ray spectrometer (EDS). Additionally, a TSL Delphi system with integrated EDS and an electron backscatter diffraction system was used to identify the phases by indexing the Kikuchi bands. The powder diffraction file, PDF-4, database was used for phase identification. To improve the reliability, only grains with a confidence index (CI) higher than 0.1 were used for the phase identifications. For comparison, a study on a face-centered cubic material has shown that the fraction of correctly indexed patterns with average CI greater than 0.1 is 95% [8].

The thermal cycles measured in all the experiments during the welding process show similar results; therefore, only the data set from one experiment will be shown in the current study, as presented in Figure 2. At the first stage (sleeve plunging), the temperature increases drastically to a peak temperature of approximately 450 °C and then falls to 370 °C. Subsequently, the temperature again increases to approximately 432 °C, before declining to approximately 412 °C. At the second and third stages (the dwell and sleeve retraction periods), it appears that the temperature follows an increasing trend to 440 °C with both lower heating and cooling rates, as shown in the inset in Figure 2. Although the material flow was different during the dwell and sleeve retraction periods, the temperature cycle in both periods remained unchanged. During the sleeve retraction period, the pin extrudes the softened material. Finally, after the fourth stage (the surface dwell period) the temperature decreases to room temperature.

A low-magnification overview of the quenched sample is shown in Figure 3a. Some material was extruded into the cavity left by the pin. Cracks across the weld center can be observed. These cracks were generated during the removal of the sleeve from the quenched sample, most likely along the brittle phase boundaries. A higher-magnification image of the area marked with a rectangle in Figure 3a is presented in Figure 3b. The microstructure consists of two types of structures, named A and B. Structure A is a gray phase, whereas structure B has a eutectic structure composed of both gray and dark phases. The qualitative chemical analysis with EDS shows that the gray phase in structure A is composed of 61 wt.% Mg and 39 wt.% Al, while structure B is 68 wt.% Mg and 32 wt.% Al. According to the Al–Mg phase diagram [9], the phases in structures A and B correspond to the $Al_{17}Mg_{12}$ and eutectic structure, containing both $Mg_{17}Al_{12}$ and α-Mg, respectively.

In the first stage of the process (sleeve plunging), the temperature increases drastically to a peak temperature of 450 °C with a heating rate of approximately 285 °C s^{-1}, as observed in Figure 2. During frictional heating, the plasticized Mg material was extruded toward the Al sheet in the weld center, and some Mg was also moved into the Al top sheet. When the composition of the Al–Mg reached the composition of the eutectic structure, a liquid phase was formed locally because the eutectic structure has the lowest solidus temperature in the Al–Mg phase diagram [9].

Several studies have demonstrated the formation of intercalated layers of base material in the stir zone of the friction stir spot welds [10,11]. Accordingly, this means that the interfacial area between both base materials is greater. During high-temperature exposure, interdiffusion of Al and Mg atoms occurred at the interface. Hence, the extension of the interfacial area between Al and Mg enhances the overall diffusion rate in the welded area [4]. It is also well known that friction-based joining produces a weld possessing a stir zone with a high density of low-angle grain boundaries and a fine grain structure due to the intense plastic deformation and high-temperature exposure [12–14]. A low-angle

Table 1. The chemical composition in wt.% of Mg alloy AZ31 and Al AA5754.

Material	Al	Mg	Fe	Zn
AZ31	2.52	Balance	–	2.03
AA5754	Balance	3.66	0.59	0.43

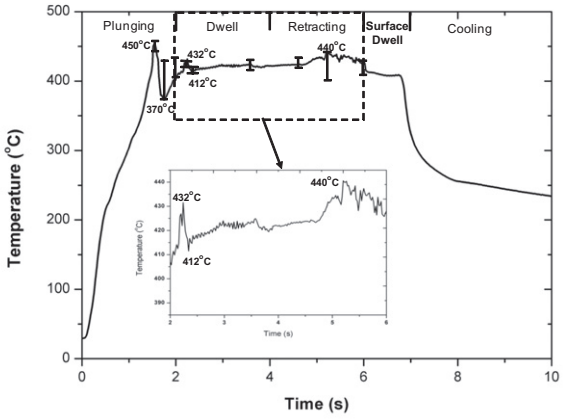

Figure 2. The temperature profile during the friction spot welding. The scattering of the key temperatures is shown in the diagram.

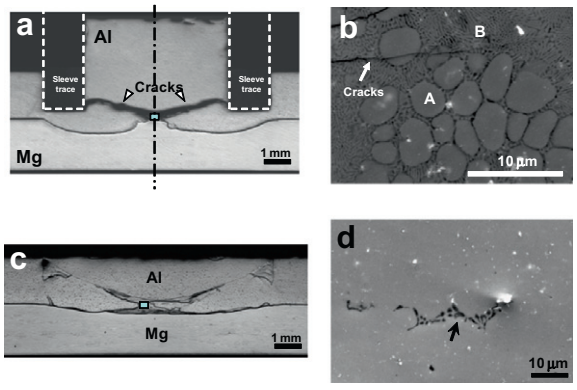

Figure 3. A low-magnification overview of the quenched sample (a) and the welded sample (c); and a micrograph taken from the weld center, as marked in (a) and (c), for (b) and (d), respectively.

boundary is characterized as a boundary with a misorientation angle of less than 15°, while a high-angle boundary exhibits a misorientation angle higher than 15°. The presence of grain boundaries is associated with a more open structure in which the migration of atoms along the grain boundaries is easier than the diffusion of atoms through the lattice [15]. Therefore, material with a finer grain size should have a higher diffusion rate than material with a larger grain size.

Both the increased interfacial area and grain boundary area, which are induced by the intense plastic deformation and high-temperature exposure, enhance the diffusion rate. Therefore, the diffusion rate during welding, carried out with intense plastic deformation, should be higher than that in a condition without it, which is in agreement with a previous study by Yasan et al. [16], which investigated the friction welding of Al/316 stainless steel. Generally, the interfacial diffusion plays an important role in enhancing the diffusion rate, and this role is larger than that of grain boundary diffusion [15]. However, the total grain boundary area including high- and low-angle boundaries should be much larger than the total interfacial area of the Al and Mg alloys at the intercalated layer. Therefore, it is likely that the grain boundary diffusion will become a dominant factor affecting the entire diffusion rate [15].

The formation of the local molten material led to a decrease in the viscosity of the plasticized material, and in this case, no frictional heating was generated, which drastically affected the heating rate. Hence, the temperature declined significantly to 370 °C with a cooling rate of approximately 390 °C s^{-1}, as shown in Figure 2. However, when the local molten material had solidified, the viscosity of the plasticized material increased, and frictional heating was once more generated. The temperature then increased to 432 °C with a heating rate of approximately 120 °C s^{-1}. The heating and cooling processes occurred repeatedly such that the peak temperature attained during FSpW corresponds to the solidus temperature of the eutectic structure. It should be noted that the temperature fluctuations produced thereafter were not as high as before, while the temperature baseline increased to 440 °C, as observed in the inset in Figure 2. Most likely, this observation corresponds to an extension of the eutectic-liquid phase, which might have stabilized the peak temperature accordingly. The extension of the eutectic-liquid phase is a result of the intense, continuous interdiffusion that occurs. During quenching, the phase transformed into the eutectic structure, as observed in Figure 4a. However, further investigation is required here.

Figure 3c shows a low-magnification overview of the welded sample. The gray and dark layers were formed at the Al and Mg interfaces, mostly in a region around the weld center and also in several regions within the Al sheet. In the current study, however, only the gray phase present in the weld center will be discussed. The microstructure of the gray layer as analyzed in the region indicated by rectangle in Figure 3c is presented in Figure 3d.

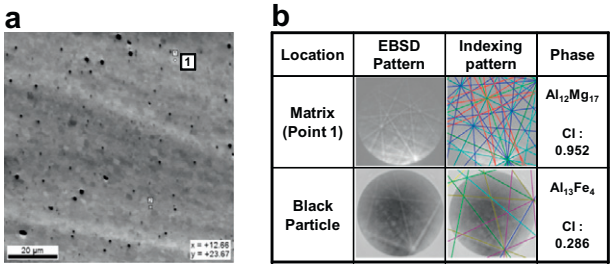

Figure 4. A forescatter image (a), and phase identification using TSL Delphi (b).

This region consists of a gray phase, a eutectic structure (indicated by an arrow) and white particles, as shown in Figure 3d. The EDS results reveal that the gray phase has a lower Mg content of 57 wt.% and 43 wt.% Al, while the white particle has a high content of Fe (~29 wt.%). The forescatter image of the gray phase reveals that the microstructure consists of fine equiaxed grains and small black particles (or white particles in the SEM image in Fig. 3d), as shown in Figure 4a. The phase identification of several of these grains by TSL Delphi reveals that the gray phase is $Al_{12}Mg_{17}$, which has a cubic crystal structure, and that the black particles are $Al_{13}Fe_4$, which has an orthorhombic crystal structure, as presented in Figure 4b.

During the sleeve retraction process, further intense interdiffusion occurred, induced by the plastic deformation and the temperature exposure, and resulted in a high content of fine $Al_{12}Mg_{17}$ grains, as observed in Figure 4a. It is likely that the fine grain structure of the $Al_{12}Mg_{17}$ was formed due to the recrystallization process, which commonly occurs in friction-based joining processes [12–14]. It is important to note that the fraction of the eutectic structure present in the weld center is smaller when compared to that observed in the quenched sample. The redistribution of the liquid phase during the extrusion process and the decomposition of the eutectic structure induced by the intense diffusion are most likely the significant factors contributing to the different fractions of the eutectic structure.

The formation of $Al_{13}Fe_4$ has not been previously mentioned in the dissimilar welding of Al and Mg alloys. These particles could be observed in the AA5754 base material. However, it should be noted that AA5754 base material exhibits large, irregular $Al_{13}Fe_4$ particles, while at the weld zone they have a spherical shape. One possible reason for this is that the large, irregular $Al_{13}Fe_4$ particles in the base material became spherical due to deformation during the welding process [17]. Another possibility was proposed by Blosmo et al. [18]. The authors used Thermocalc software to perform thermodynamic and phase diagram calculations for multicomponent systems to predict the compounds that might form during the dissimilar welding of Al/Mg alloys. The authors reported that several phases, including $Al_{13}Fe_4$, could be formed at a temperature of 327 °C. Because the maximum measured temperature during welding is much lower than the melting point of the $Al_{13}Fe_4$, which is approximately 1160 °C [19], it is likely that $Al_{13}Fe_4$ particles form due to the diffusion process. Although the base material contains $Al_{13}Fe_4$ particles, there is a possibility that new $Al_{13}Fe_4$ particles were also formed during the welding process. However, this requires further investigation.

In the present study, the thermal cycling behavior during the dissimilar friction spot welding of AA 5754/AZ31 was measured. At the beginning of the process, due to the frictional heating, the weld is heated to a peak temperature of 450 °C, which is higher than the equilibrium solidus temperature of the eutectic structure. The plastic deformation and high-temperature exposure induced the grain boundary diffusion and the interfacial diffusion, thus local melting occurred. Liquefaction and solidification occurred repeatedly, resulting in a non-equilibrium solidus temperature. During the sleeve retraction period, the "solid–liquid" phase material experienced further diffusion and dynamic recrystallization, resulting in the formation of the fine equiaxed $Al_{17}Mg_{12}$ grains at the weld center.

The authors gratefully acknowledge Mr. F. Kroeff for technical assistance, Dr. Rene de Kloe from EDAX BV Tilburg for the phase identifications, and Dr. J. Shen for helpful discussions.

[1] C. Schilling C, J.F. dos Santos, Method and Device for Linking at Least Two Adjoining Work Pieces by Friction Welding. European Patent EP 1230062 B1 (WO 2001/036144), 1999.
[2] T. Rosendo, B. Parra, M.A.D. Tier, A.A.M. da Silva, J.F. dos Santos, T.R. Strohaecker, N.G. Alcantara, Mater. Des. 32 (2011) 1094.
[3] L.C. Campanelli, U.F.H. Suhuddin, J.F. dos Santos, N.G. Alcantara, Mater. Sci. Forum 706–709 (2012) 3016.
[4] Y.S. Sato, S.H.C. Park, M. Michiuchi, H. Kokawa, Scripta Mater. 50 (2004) 1233.
[5] A. Gerlich, P. Su, T.H. North, Sci. Technol. Weld. Joining 10 (2005) 647.
[6] A. Kostka, R.S. Coelho, J. dos Santos, A.R. Pyzalla, Scripta Mater. 60 (2009) 953.
[7] Y.C. Chen, K. Nakata, Scripta Mater. 50 (2008) 433.
[8] TSL OIM version 5.31 On-line help.
[9] ASM Metals Handbook, in: Alloy Phase Diagrams, vol. 3, Materials Park, OH, ASM International, 1992.
[10] P. Su, A. Gerlich, T.H. North, G.J. Bendzsak, Metall. Mater. Trans. A 38A (2007) 584.
[11] P. Su, A. Gerlich, M. Yamamoto, T.H. North, J. Mater. Sci. 42 (2007) 9954.
[12] J. Jeon, S. Mironov, Y.S. Sato, H. Kokawa, S.H.C. Park, S. Hirano, Acta Mater. 59 (2011) 7439.
[13] U.F.H.R. Suhuddin, S. Mironov, Y.S. Sato, H. Kokawa, Acta Mater. 57 (2009) 5406.
[14] P.B. Prangnell, C.P. Heason, Acta Mater. 53 (2005) 3179.
[15] D.A. Porter, K.E. Easterling, Phase Transformations in Metals and Alloys, Van Nostrand Reinhold, Wokingham, 1981.
[16] D. Yashan, S. Tsang, W.L. Johns, M.W. Doughty, Weld. J. 66 (1987) 27.
[17] K. Nakata, Y.G. Kim, H. Fujii, T. Tsumura, T. Komazaki, Mater. Sci. Eng. A 437 (2006) 274.
[18] D.J. Blosmo, T. Curtis, T. Johnson, N. Procive, C.A. Widener, B. Carlson, R. Szymanski, M.K. West, in: R. Mishra, M.W. Mahoney, Y. Sato, Y. Hovanski, R. Verma (Eds.), Friction Stir Welding and Processing VI, Warrendale, PA, TMS, 2011, p. 409.
[19] R. Hultgren, P.D. Desai, D.T. Hawkins, M. Gleiser, K.K. Kelley, D.D. Wagman (Eds.), Selected Values of the Thermodynamic Properties of the Elements, ASM International, Materials Park, OH, 1973.